Location of Critical Slip Surfaces in Coal Mine Spoil Piles

D.J. WILLIAMS
B.E., Ph.D., M.I.E.Aust.
Senior Lecturer in Civil Engineering, The University of Queensland
J.-Z. ZOU
B.E., M.E.
Research Student, The University of Queensland

SUMMARY By their very nature, coal mine spoil piles are at considerable risk of instability. The stresses within a coal mine spoil pile of a particular geometry are calculated using the stochastic finite element method, which allows for the observed variability of the spoil material properties. Various base spoil strengths are adopted to demonstrate the sensitivity of the results to conditions in this critical region. Using the calculated stresses, an improved dynamic programming method is used to locate the critical slip surface within the spoil pile, and hence determine the minimum factor of safety, for each set of spoil material strengths. The minimum factors of safety obtained are compared with those determined using a generalised limit equilibrium wedge analysis employing a pattern search optimisation procedure. Possible improvements to the stochastic finite element based improved dynamic programming method are discussed.

1. INTRODUCTION

In Australia, the spoil removed to expose coal during surface mining is conventionally loose dumped from a dragline bucket in spoil piles within the already mined pit. Since the spoil is free to ravel at about its angle of repose (of the order of 37 ° to the horizontal) and water softened material can occur at the base, there is a considerable risk of spoil pile instability. Investigations by others (1, for example) of the failure of coal mine spoil piles have revealed that the failures are characterised by a deep-seated, essentially two-wedge mechanism, in which the pit floor region forms the base of the lower wedge, and the upper wedge extends behind the latest spoil pile crest. The failures extend to the pit floor region either because of water softened spoil at that location, or because of the presence of a weak seam within the floor material. In this paper, failure confined to the spoil only will be considered, and pore water pressures are absent from the spoil pile.

The precise location of the critical slip surface within a spoil pile is best determined by some optimisation procedure. One such procedure is the dynamic programming method. In this method, the distribution of stresses within the spoil pile is required. This may be provided by finite element calculations, which allow a constitutive model for the spoil material to be incorporated into the solution. The geotechnical properties of spoil material vary considerably, and this was allowed for by employing a stochastic finite element method (2). Definition of the variability of the spoil material properties was based on a simple statistical analysis of spoil property data collected from coal mines in the Bowen Basin Coalfields in Central Queensland. The geometry of the spoil pile can also vary markedly. However, for the purposes of the paper a particular spoil pile geometry was adopted. In the stochastic finite element calculations, various values for the strength parameters at the critical base of the spoil pile were considered to demonstrate the sensitivity of the solution to conditions at the spoil base.

Use of the dynamic programming method requires the definition of a grid of state points which overlaps the potential slip region. The state points are arranged in a series of stages. An improved dynamic programming method was used, in which possible slip surfaces, which must pass between state points, may pass both between and along stages. In the conventional dynamic programming method, slip surfaces may only pass between stages (3). Allowing possible slip surfaces to pass both between and along stages has the potential to provide greater accuracy for a given spacing of state points. The critical slip surface is that which gives the minimum factor of safety.

The results obtained using the improved dynamic programming method are compared with the results obtained using a generalised limit equilibrium wedge analysis employing a pattern search optimisation procedure (4). The accuracy of and possible improvements to the stochastic finite element based improved dynamic programming method are discussed.

2. SPOIL PILE GEOMETRY

Although the geometry of spoil piles varies greatly, depending among other factors on the depth to coal, the lithology and breakdown potential of the spoil, the mining methods employed and the dip of the coal seam, a fixed geometry was adopted for the purposes of this paper. It was based on that analysed by Richards (5), as used by Williams and Zou previously (2), and is shown in Figure 1. It involves a spoil pile 76.5 m high, with a slope face angle of 34.5 ° and a base slope angle of 3.4 °. Behind the leading face is a series of 20 m high crests with 37 °slopes. The height of the spoil pile is about the maximum achieved by spoil piles, and it has a relatively steep face angle, so that it represents somewhat of a worst case. The spoil pile is assumed to be located on strong floor material, so that any failure would occur entirely within the spoil. Pore water pressures are absent from the spoil pile.

3. MATERIAL PROPERTIES

3.1 Results of Statistical Analyses of Collected Spoil Property Data

Spoil materials produced by the surface mining of coal in the Bowen Basin Coalfields of Central

Queensland comprise soil and uncemented "superficials", and coal measures overburden and interburden rocks. Data on the density ρ and strength of these materials were collected from records of spoil pile failure investigations carried out at Goonyella and Riverside Mines, and from records of laboratory and in situ testing of spoil materials from these mines.

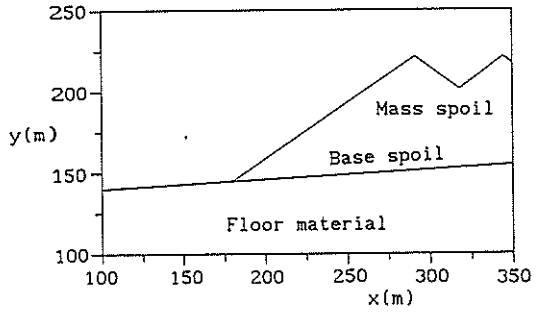

Figure 1 Adopted spoil pile geometry

Borehole samples taken from basal failure zones show the existence, in some cases, of a band of highly saturated softened spoil at the pit floor/spoil interface. Therefore, it is appropriate to consider data on the base spoil strength separately from spoil mass strength data.

The available strength data was based on the confined triaxial testing of a range of spoil materials, under various test conditions. The data exhibited a large variability, but it was not possible to separate the data according to lithology and the potential for material breakdown, nor according to test conditions. In practice, little attempt is made to selectively place spoil of different strength in order to optimise stability, apart from some selective placement of good quality spoil at the critical base of the pile. The available spoil strength data comprised values of mass and base cohesion (c_m and c_b, respectively), and values of mass and base friction angle (ϕ_m and ϕ_b, respectively).

The statistical analyses of the spoil density and strength data were carried out using a commercially available computer package SAS. The results of the analyses are summarised in Table I.

TABLE I

RESULTS OF STATISTICAL ANALYSES OF COLLECTED SPOIL DENSITY AND STRENGTH DATA

Spoil property	Data set size	Mean μ	Standard deviation σ
ρ ($Mg.m^{-3}$)	61	1.86	0.22
c_m (kPa)	62	73.1	77.7
ϕ_m ($^\circ$)	62	28.1	10.8
c_b (kPa)	87	121.8	83.1
ϕ_b ($^\circ$)	87	8.0	4.0

The standard deviations given in Table I show that the cohesion data are widely scattered in both absolute and percentage terms. The scatter of the density and ϕ_m data is small, while the scatter of the ϕ_b data, although large in percentage terms, is only moderate in absolute terms.

All of the spoil properties other than c_m may reasonably be approximated as being normally distributed. The distribution of c_m is somewhat better approximated by an exponential or log-normal distribution. However, for the purposes of the paper, all spoil properties were assumed to be normally distributed. In the ensuing analyses, three sets of spoil strengths were considered. In the first, the spoil strengths given in Table I were adopted. In the second, zero cohesion (mean and standard deviation) was assigned for the base spoil, and in the third zero friction angle (mean and standard deviation) was assigned to the base spoil, with the other strengths unchanged from those given in Table I. Assigning zero friction angle to the base spoil may be thought of as representing undrained failure at the base.

3.2 Other Material Properties

To apply the stochastic finite element method, values for a number of other properties are required. These properties include the strength of the floor material, the Young's moduli of the spoil and floor materials, and the Poissons ratio of the spoil and floor materials. Mean values for the cohesion and friction angle of the floor material were taken to be 625 kPa and 28°, respectively, after Richards (5). Mean values for the Young's modulus of the floor material beneath the spoil, mass spoil material, and base spoil material were estimated from modulus data given in Richards (5) to be 154 MPa, 28 MPa and 19 MPa, respectively. A value of 0.3 was assumed for the Poissons ratio of all materials. No data were available on the distributions of these properties, and zero standard deviations were adopted.

4. STOCHASTIC FINITE ELEMENT METHOD

4.1 Introduction

The stochastic finite element method (SFEM) is an extension of the conventional finite element method (FEM) to reliability analysis. The SFEM uses as input the probability distributions of the spoil material properties, rather than the deterministic values used in the conventional FEM. The probability distributions of the stresses and displacements within a body are then calculated by approximate methods as outlined in Williams and Zou (2). For this paper use was made of a SFEM program developed from a general purpose finite element program written by Owen (6). The program can be used for reliability analyses of problems that involve elasto-plastic work-hardening material behaviour. This represents an advance on available SFEM programs which cater for elastic material behaviour only.

4.2 Application of SFEM to Spoil Pile Stability Analysis

Since the probability distributions of the spoil material properties have been approximated as normal, they are defined by the means and standard deviations of the spoil material properties, and these are used as input to the SFEM program. The program then calculates the means of the stresses and displacements, and their standard deviations, throughout the spoil pile. The stresses are used as input in the application of the improved dynamic programming method.

The SFEM program also compares the calculated stresses with the adopted yield criterion, to give the probability of failure and factor of safety locally. The location of high values of the local probability of failure or low values of the local factor of safety within the spoil pile indicates

the probable location of the critical slip surface. This is used as a basis for selecting the appropriate location for the state point grid used in the improved dynamic programming method.

As described in Williams and Zou (2), the spoil pile geometry shown in Figure 1 was represented by a finite element mesh comprising 74 eight-noded iso-parametric plane strain elements. It was assumed that the spoil material and underlying floor material would behave as if they were fully drained. They were therefore modelled as single phase materials, with only two degrees of freedom (the horizontal and vertical components of displacement) assigned to each node. Both the horizontal and vertical nodal displacements were constrained to zero at the base of the mesh. The horizontal displacement component only was constrained to zero at the vertical boundaries of the mesh. The strength properties of the spoil at the base of the pile, different from that of the spoil mass, were modelled by assigning different strength properties to a 1 m thick layer at the spoil pile base.

Both the spoil and floor materials were modelled as isotropic materials, characterised by linear elastic behaviour until the yield point, which was defined by the Mohr-Coulomb criterion. Beyond yield, the material was allowed to undergo work-hardening defined by a hardening parameter equal to one tenth of the relevant Young's modulus, following the approach taken by Owen (6). The incorporation of work-hardening was necessary to ensure a convergent solution in cases close to failure.

4.3 Results of SFEM Analyses

For the purposes of calculating local probabilities of failure and factors of safety, the Mohr-Coulomb yield criterion was used in a performance function, as detailed in Williams and Zou (2). Contours of the local probability of failure for the three sets of spoil strengths considered were presented as Figures 2, 3 and 4 in (2), and will not be repeated here. They served as a basis for selecting the appropriate location for the state point grid used in the improved dynamic programming method.

5. IMPROVED DYNAMIC PROGRAMMING METHOD

5.1 Introduction

Dynamic programming has been developed as a numerical algorithm for the rapid optimisation of sequential multi-stage decision problems (3, 7). Such problems are characterised by two features. Firstly, that at any stage the system may exist in any one of a finite number of states and, secondly, that it is required to find the mimimum system "cost". The minimum cost depends on the trajectory between stages and is defined as the sum of the costs incurred on passing between adjacent stages. The problem of determining the critical slip surface and hence mimimum factor of safety of a slope may readily be formulated in this manner. In this paper, an improved dynamic programming method (IDPM) is employed, in which possible slip surfaces can pass both between and along stages.

The application of the dynamic programming method requires that it be coupled with an appropriate analysis for the solution of the problem in question. Baker (3) described a procedure for applying the dynamic programming method, coupled with Spencer's limit equilibrium method of slope stability analysis, to locate the critical slip surface and hence determine the mimimum factor of safety. Yamagami and Ueta (8) applied the dynamic programming method, coupled with an expression for the factor of safety, to search for critical slip surfaces in finite element stress fields. In this paper, the IDPM is coupled with an expression for the factor of safety in which the stresses are obtained from stochastic finite element calculations. The IDPM is described briefly and used to locate the critical slip surface and hence determine the minimum factor of safety of a coal mine spoil pile, for three different sets of strength parameters.

5.2 Equations for Factor of Safety and Incorporation into Dynamic Programming

Similar to the approach taken by Yamagami and Ueta (8), the overall factor of safety for a particular slip surface (such as curve AB in Figure 2) can be defined as

$$F_s = \frac{\int_A^B \tau_f . dx}{\int_A^B \tau . dx} = \frac{\sum_{i=1}^{n} \tau_{f_i} . \delta l_i}{\sum_{i=1}^{n} \tau_i . \delta l_i} \qquad (1)$$

where τ is the mobilised shear stress at any point along the slip surface AB, τ_f is the shear strength of the material at that point, x is the horizontal co-ordinate, n is the number of stages along the slip surface, and δl_i is the length of the ith stage.

Dynamic programming is applicable only to "additive" integration functions or summations (3), which are merely numerical approximations to linear functions. Since the expression for the factor of safety given by equation (1) involves a ratio of integration functions or summations, it is not additive as required. This can be resolved using the principles of variational calculus, by introducing an auxiliary functional G_F defined by the following expression.

$$G_F = \sum_{i=1}^{n} (\tau_{f_i} - F_s . \tau_i) . \delta l_i \qquad (2)$$

Equation (2) is an additive function to which dynamic programming may be applied. Baker (3) showed that by minimising G_F, the minimum value for F_s would be obtained.

For the ith stage on a particular slip surface, the following expressions for τ_{fi} and τ_i can be written.

$$\tau_{f_i} = c + \sigma_s . \tan\phi \qquad (3)$$

$$\tau_i = \frac{(\sigma_1 - \sigma_3)}{2} . \sin(2\beta) \qquad (4)$$

where c is the cohesion and ϕ the friction angle of the material comprising the slope, σ_s is the stress acting normal to the slip surface over the ith stage, and σ_1 and σ_3 are the major and minor principle stresses at the slip surface over the ith stage, respectively. Equation (3) is the Mohr-Coulomb yield criterion. The stress σ_s and the angle β are given by the following expressions.

$$\sigma_s = \frac{(\sigma_1 + \sigma_3)}{2} + \frac{(\sigma_1 - \sigma_3)}{2} . \cos(2\beta) \qquad (5)$$

$$\beta = \alpha - \vartheta + \frac{\pi}{2} \qquad (6)$$

where α is the angle the base of the ith stage makes with the horizontal, and θ is the angle σ_1 makes with the horizontal.

In optimising equation (2) for each slip surface selected within the defined grid of state points, a value for F_s is first assumed. During the optimisation process, equation (1) is used to calculate a value for F_s and the result compared with the assumed value. The assumed value for F_s is updated and the process continued until some convergence criterion (such as the assumed and calculated values of F_s agreeing to within 0.01) is reached.

5.3 Brief Description of IDPM

The region of possible slip surfaces is selected using the results of stochastic finite element calculations as a basis. Within this region a grid of state points is arranged comprising n stages, with j state points along the ith stage line (such a grid is shown in Figure 2). Each state point, represented by S(i,j), has a certain value for its state parameter (or stress state). For state points outside the slope, the state parameter is zero. The state parameters for state points within the slope are based on the results of stochastic finite element calculations. The "cost" between any two state points can be calculated based on their separation distance and the difference in value of their state parameter. The minimum cost between the initial state point S(1,1) and any state point S(i,j) is defined by the optimal value function H(i,j).

There is a restriction in the application of dynamic programming that all trajectories pass through fixed end points, which implies that H(1,1) and H(n+1,1) have one value each. Provided that these fixed end points are located outside the slope, where the state parameter is zero, this restriction is of no practical concern.

For a given slope geometry, given slope material properties, and a defined region of possible slip surfaces, the following summarises the IDPM procedure for locating the critical slip surface and determining the corresponding minimum factor of safety.

1. The optimal value function of the starting point (state point S(1,1) or point A in Figure 2) is initialised to zero, that is

$$H(1,1) = 0 \qquad (7)$$

2. A value is assumed for the optimal value function of the ending point (state point S(N+1,1) or point B in Figure 2). Then, based on the recurrence relation derived from Bellman's (7) optimisation principle, the optimal value function for each state point of each stage line may be calculated (3). In this step, the optimal value functions for all possible paths from each stage point, both between and along stages, are calculated.

3. The optimal value function of the ending point is minimised.

4. The critical slip surface is traced back through the possible slip surface region, based on the calculated minimum optimal value functions, and hence the minimum factor of safety determined.

According to Giam and Donald (9), in a perfect state point grid the stage lines should be perpendicular to the critical slip surface. However, the one state point grid must suffice for all possible slip surfaces. As the critical slip surface is the most important, a check should be made that it intersects the stage lines approximately at right angles everywhere. The benefits of the IDPM over the conventional dynamic programming method, in which possible slip surfaces can only pass between stage points on adjacent stages, becomes more marked the more acute the angle between the slip surface and the stage lines.

5.4 Application of IDPM to Spoil Pile Stability Analysis

Based on the results of the SFEM analyses, the state point grid shown in Figure 2 was selected. The state points were arranged in a series of stages, with stages on average 2 m apart and state points within each stage on average 0.55 m apart. This gave a state point grid about one order of magnitude finer than that used for the same spoil pile geometry by Williams and Zou (2). For convenience in setting up the geometry of the state point grid, which was generated automatically, it extends beyond the slope boundary. All state points outside the spoil pile are assigned zero state parameters. The stress state at each state point within the spoil pile represents the local stress state of its surrounding area, and was assigned the stress calculated for the finite element Gauss point nearest to the particular state point. Possible slip surfaces are formed by connecting fixed points A and B (Figure 2), outside the slope, via intermediate state points. The only state points of any consequence are those located within the slope. It can be seen that the slip surface intersects the stage lines approximately at right angles everywhere.

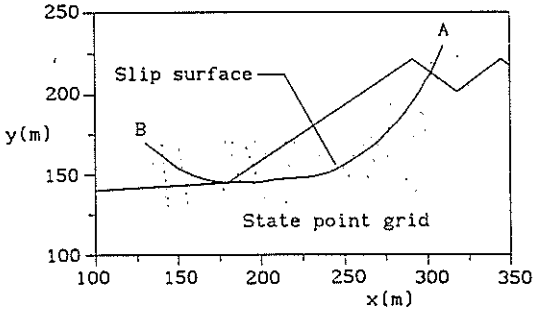

Figure 2 Selected state point grid showing slip surface AB

5.5 Results of IDPM Analyses

The results of the stochastic finite element based IDPM analyses are shown in Figures 3, 4 and 5, for the mean spoil strengths given in Table I, zero base spoil cohesion and zero base spoil friction angle, respectively. Figures 3 to 5 show the locations of the critical slip surface and the values of the minimum factor of safety obtained.

6. GENERALISED WEDGE ANALYSIS

6.1 Introduction

The generalised limit equilibrium wedge analysis program GWEDGEM, described in Donald and Giam (4), was used for the purposes of comparison with the results obtained using the SFEM and IDPM. In GWEDGEM, both force and moment equilibrium are fully satisfied and the failure mechanism is kinematically admissible. That is, the sliding

wedges may move without causing gaps or overlaps. Inclined internal interfaces are allowed and the critical inclination is searched for. Various multi-variable unconstrained search routines are available within the program for locating the critical slip surface for a given problem. The mechanism may have any multi-linear shape, although two to nine wedges are usually sufficient. The method is applicable to general stability problems, and has been shown (4, 10) to be superior to available limit equilibrium methods employing vertical slices, where the critical slip surface is non-circular.

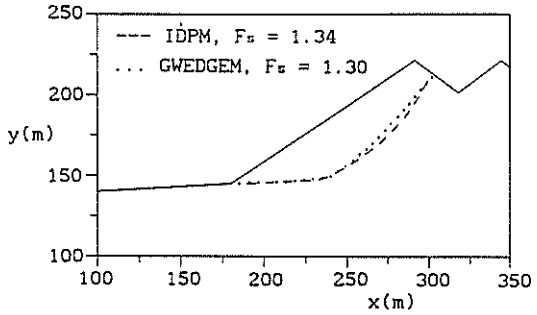

Figure 3 Critical slip surfaces and minimum factors of safety F_s for mean spoil strengths

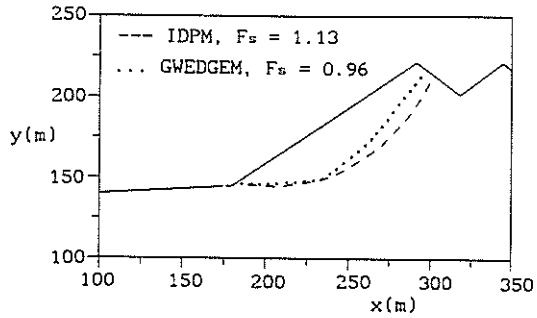

Figure 4 Critical slip surfaces and minimum factors of safety F_s for zero base spoil cohesion

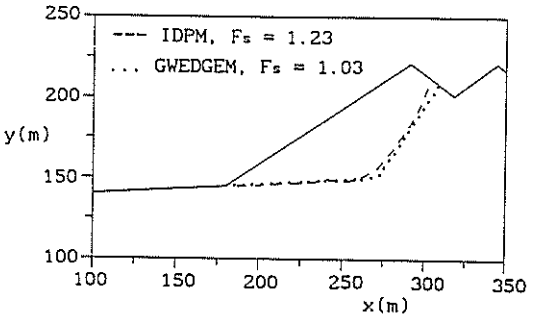

Figure 5 Critical slip surfaces and minimum factors of safety F_s for zero base spoil friction angle

In view of the relatively tight curvature of the critical slip surface, nine wedge mechanisms were selected. The pattern search option was adopted as the optimisation procedure for the determination of the critical slip surface for the three sets of strength parameters. The pattern search procedure was found by Giam and Donald (9) to be one of the best options available within GWEDGEM. It can successfully handle a wide range of slope stability problems, the number of slip surfaces needed to be considered to arrive at the minimum factor of safety is not excessive, and it is computationally efficient.

6.2 Results of GWEDGEM Analyses

The results of the limit equilibrium based GWEDGEM analyses are shown together with the results of the corresponding IDPM analyses in Figures 3, 4 and 5. Figures 3 to 5 show the locations of the critical slip surface and the values of the minimum factor of safety obtained.

7. DISCUSSION

The minimum factors of safety F_s obtained from the two analyses used in this paper, and from earlier IDPM analyses for the same spoil pile geometry and spoil material properties by Williams and Zou (2), are compared in Table II.

TABLE II

COMPARISON OF CALCULATED MINIMUM FACTORS OF SAFETY

Spoil strengths	Minimum F_s		
	IDPM		GWEDGEM
	(2)	Current	
Mean strengths	1.79	1.34	1.30
Zero base cohesion	1.16	1.13	0.96
Zero base friction	1.42	1.23	1.03

7.1 Effect of State Point Grid Spacing

The disparity between the minimum F_s calculated in the current IPDM analyses and those reported in (2), are due to the state point grid spacing being about an order of magnitude finer in the current analyses. The inadequacy of this spacing was evident from the jagged critical slip surfaces which were obtained.

Figures 3 to 5 show the critical slip surfaces obtained to be reasonably smooth, and the minimum F_s obtained were substantially reduced. Using the mean base spoil strengths, the finer spacing resulted in a 34 % reduction in the calculated minimum F_s. For zero base spoil cohesion the reduction was only 3 %, while for zero base friction angle the reduction was 15 %. It appears that the higher the overall strength of the base spoil, the finer the state point grid spacing required to achieve acceptable accuracy, particularly where the resistance at the base is mainly cohesive. Where the resistance at the base is mainly frictional, a relatively coarse state point grid appears adequate.

7.2 Effect of Base Spoil Strength

The minimum F_s values determined in the current IDPM and GWEDGEM analyses both demonstrate the critical part played by the strength of the spoil at the base of the pile in providing stability. The GWEDGEM results show that removing either the base spoil cohesive or frictional resistances reduces the minimum F_s value to about unity. Considering the relative orders of magnitude of the two strength components, base frictional resistance has a relatively larger effect than does base cohesion.

Figures 3 to 5 show that while the removal of base spoil cohesion has little effect on the location of the critical slip surface, the removal of base spoil frictional resistance lengthens the basal

plane and steepens the back slope of the critical slip surface considerably. This has the effect of involving a greater volume of spoil in a potential failure.

7.3 Comparison of Current IDPM and GWEDGEM Results

Figures 3 to 5 show that the current IDPM and GWEDGEM analyses give similar locations for the critical slip surfaces. For the mean spoil strengths, the two analyses gave comparable minimum F_s values. However, for zero base spoil cohesion and zero base spoil friction angle, the GWEDGEM analyses gave considerably lower minimum F_s values (about unity) than the IDPM analyses.

These results appear to be mainly attributable to the effect of work-hardening in the SFEM. Since the mean spoil strengths gave a minimum F_s value well above unity, little of the spoil pile material would have yielded and subsequently work-hardened. Hence, similar minimum F_s values were obtained by the two analyses. A separate analysis with no work-hardening in the SFEM gave an almost unchanged minimum F_s value of 1.33 for the mean spoil strengths. However, the other two sets of spoil strengths brought the minimum F_s value close to unity. Under these conditions, a considerable amount of the spoil material in the vicinity of the slip surface would have yielded and the effect of the imposed work-hardening was to raise the apparent minimum F_s value. Attempted SFEM analyses without work-hardening failed to converge for these two cases.

7.4 Possible Improvements to IDPM Analysis

Refinement of the work-hardening function in the SFEM is required to avoid it causing an excessive rise in the minimum factor of safety, particularly when the minimum value approaches unity. Further investigation is warranted of the state point grid spacing required for different spoil pile geometries and spoil material strengths. Refinement of the way in which state point stresses are determined from finite element calculations is warranted. Yamagami and Ueta (8) found that there could be a significant difference in the minimum factor of safety obtained depending on how state point stresses were approximated.

8. CONCLUSIONS

The coupling of numerical optimisation techniques with stability analyses or computed stress fields has been the subject of a number of papers over the last decade. This paper adds another variant, with the use of the stochastic finite element method to calculate the stress field, and the use of an improved dynamic programming method to locate the critical slip surface. This advance is aimed at allowing for the constitutive behaviour and variability of geomaterials and improving computational efficiency.

As advances are made there is a continual need to check the results produced against more proven methods. The critical slip surface and corresponding minimum factor of safety for a coal mine spoil pile has been obtained using the new method for three sets of spoil material strengths. The results obtained have been compared with those of a proven generalised limit equilibrium based wedge analysis employing a pattern search optimisation procedure. The comparison showed good agreement in the location of the critical slip surfaces, but showed some disagreement in the minimum factors of safety obtained. Reasons for this have been suggested, highlighting features of the new method which warrant further attention.

9. ACKNOWLEDGEMENTS

The authors are indebted to the late Peter Giam and to Ian Donald for providing access to the program GWEDGEM. The co-operation of BHP-Utah Coal Limited in providing access to records of spoil density and strength data from Goonyella and Riverside Mines is gratefully acknowledged. During the course of the research work on which this paper is based, the second named author was partially supported by a National Energy Research Development and Demonstration Council grant.

10. REFERENCES

1. Boyd, G.L., Komdeur, W. and Richards, B.G. (1978). Open strip pitwall instability at Goonyella Mine - causes and effects. Proc. Aust. I.M.M. Conf., North Queensland, pp. 139-157.

2. Williams D.J. and Zou J.-Z. (1991). Stochastic finite element analysis of coal mine spoil pile stability. Proc. Int. Conf. of Assoc. for Computer Methods and Advances in Geomechanics, Cairns, Vol. 2, pp. 1411-1416.

3. Baker, R. (1980). Determination of the critical slip surface in slope stability computations. Int. J. for Numerical and Analytical Methods in Geomechanics, Vol. 4, pp. 333-359.

4. Donald, I.B. and Giam, S.K. (1989a). Improved comprehensive equilibrium stability analysis. Civil Engineering Research Report No. 1/1989, Monash Univ.

5. Richards, B.G. (1982). The finite element analysis of mine spoil slopes using slip elements to simulate strain softening yield behaviour. Civil Eng. Trans., I.E.Aust., Vol. CE24, No. 1, pp. 69-76.

6. Owen, D.R.J. (1980). Finite elements in plasticity. Pineridge Press Limited.

7. Bellman, R. (1957). Dynamic programming. Princeton Univ. Press.

8. Yamagami, T. and Ueta, Y. (1988). Search for critical slip lines in finite element stress fields by dynamic programming. Proc. Sixth Int. Conf. on Numerical Methods in Geomechanics, Innsbruck, pp. 1335-1352.

9. Giam, S.K. and Donald, I.B. (1989). Appropriate optimisation techniques for failure surface determination in geotechnical stability analysis. Civil Engineering Research Report No. 3/1989, Monash Univ.

10. Donald, I.B. and Giam, S.K. (1989b). Slope stability programs review. ACADS Publication No. U256.